Available online at www.sciencedirect.com
SCIENCE DIRECT
Journal of Catalysis 236 (2005) 181–189
JOURNAL OF CATALYSIS
www.elsevier.com/locate/jcat

Ammonia decomposition over Ru and Ni catalysts supported on fumed SiO_2, MCM-41, and SBA-15

Xiu-Kai Li [a,b], Wei-Jie Ji [b,*], Jing Zhao [b], Shui-Ju Wang [c], Chak-Tong Au [a,*]

[a] *Department of Chemistry, Center for Surface Analysis and Research, Hong Kong Baptist University, Kowloon Tong, Hong Kong, China*
[b] *Key Laboratory of Mesoscopic Chemistry, Ministry of Education, Department of Chemistry, Nanjing University, Nanjing 210093, China*
[c] *Analysis and Testing Center, Xiamen University, Xiamen 361005, China*

Received 12 July 2005; revised 23 August 2005; accepted 27 September 2005

Available online 28 October 2005

Abstract

The effects of using fumed SiO_2, MCM-41, and SBA-15 as supports for Ru and Ni catalysts on ammonia decomposition were investigated. It was found that the supported catalysts on these siliceous materials are more active than those supported on ordinary silica. In general, the supported Ru catalysts are more active than the Ni catalysts, and MCM-41 is the best support material for Ru and Ni. Significant enhancement in activity was observed when the supported Ru catalysts were modified by KOH, but such effect was minimal in the cases of supported Ni catalysts. The results of N_2 adsorption and transmission electron microscopy studies revealed that the Ni particles of Ni/MCM-41(TIE) prepared by template-ion exchange (TIE) method are largely located inside the pores of MCM-41. Compared with the Ni/MCM-41(IMP) catalyst prepared by impregnation method, the Ni/MCM-41(TIE) catalyst exhibited appropriate Ni dispersion and weaker Ni/support interaction, and consequently higher catalytic activity. In terms of the remarkable changes in turnover frequency (TOF) with Ni dispersion on different catalysts, it was demonstrated that NH_3 decomposition over Ni is significantly structure sensitive. Some unique metal clusters similar to B5 active sites should be responsible for the catalytic activities. Preparation methodology has a substantial influence on metal dispersion. For the supported Ni catalysts prepared by the TIE method, the generated metal particles are very small and the constitution of unique active sites becomes unfavorable, which accounts for the apparently lower TOF values.

Keywords: Ruthenium catalyst; Nickel catalyst; Siliceous materials; Ammonia decomposition

1. Introduction

The on-site generation of hydrogen for proton-exchange membrane fuel cells (PEMFCs) is of great importance for environmental protection consideration [1]. The option of producing hydrogen directly from carbonaceous substances (e.g., methanol, methane) has limitations, because the byproduct CO_x ($x = 1, 2$) degrades the cell performance even at extremely low concentrations [2–6]. As an alternative route, the direct generation of hydrogen from ammonia decomposition has been considered for the production of CO_x-free hydrogen [7–15]. On the other hand, NH_3 decomposition is a more economical method, and NH_3 storage and delivery can be more readily handled [16,17].

As for the research on NH_3 decomposition, most of the work has been related to NH_3 synthesis and/or NH_3 abatement [18–27]. There are reports on H_2 generation from pure NH_3 [19–26]; however, catalytic activity is low even at 873 K. Many metals, alloys, and compounds with noble metal characters have been tested for ammonia decomposition [8,11,13,28–36]. It was found that Ru is the most active among the noble metals, and nickel is the most active among the cheap metals. In terms of cost, Ni is attractive [15]. Supports have been used to increase the dispersion and surface area of active components. Recently, it was reported that Ru catalyst using carbon nanotubes (CNTs) as a support showed the highest activity among metal catalysts supported on various materials [30–34].

* Corresponding authors. Fax: +852 3411 7348.
E-mail addresses: jiwj@nju.edu.cn (W.-J. Ji), pctau@hkbu.edu.hk (C.-T. Au).

0021-9517/$ – see front matter
doi:10.1016/j.jcat.2005.09.030

Fumed silica is a unique kind of siliceous material comprising nonporous primary particles. It has chain-like particle morphology and porosity only between primary particles [37]. MCM-41 and SBA-15 are two important mesoporous siliceous materials synthesized by liquid crystal template (LCT) methods that have well-ordered hexagonal porosity and are high in thermal stability and surface area [38–40]. In view of the unique structural features of these siliceous materials, we envisaged that better catalytic activity could be achieved by using them as catalyst supports for ammonia decomposition. In contrast, carbon-based supports are unstable, due to methanation, in the presence of H_2 at high temperatures. The metal catalysts supported on siliceous materials should be more stable and have better prospects for practical applications.

In this work, fumed SiO_2, MCM-41, and SBA-15 were adopted as catalyst supports for ammonia decomposition, and Ru and Ni were selected as the active components. Special attention was given to the nickel catalysts, and two different methods for loading Ni were adpoted. Investigation of physicochemical properties of the catalysts was done using techniques such as X-ray diffraction (XRD), transmission electron microscopy (TEM), N_2 adsorption–desorption, H_2 temperature-programmed reduction (TPR), and H_2 temperature-programmed desorption (TPD).

2. Experimental

2.1. Catalyst preparation

Fumed silica was commercially available from Aldrich and used without any further treatment. MCM-41 and SBA-15 were synthesized by direct hydrothermal treatment according to the procedures described previously [38–40]. The loading of metal component and potassium promoter onto the supports was done by the incipient wetness impregnation method according to the procedures of Yin et al. [33]. Analytic-grade $RuCl_3$ (Aldrich) and $Ni(NO_3)_2{\cdot}6H_2O$ (Aldrich) were used as the precursors of Ru and Ni components, respectively. Acetone (for Ru and Ni loading) and ethanol (for KOH loading) were used as solvents, and KOH was used as a K precursor. The intended loading of metal component was 5 wt%; the catalysts are designated as Ru/*support*(IMP) and Ni/*support*(IMP), respectively. The KOH-modified catalysts are designated as K-metal/*support*(IMP), and the K/metal molar ratio was 2/1.

Another MCM-41-supported Ni catalyst was prepared by a template ion-exchange (TIE) method and designated as Ni/MCM-41(TIE). Typically, 2 g of as-synthesized MCM-41 containing 50 wt% template was added to an ethanol solution of nickel nitrate, and the mixture was stirred vigorously at 333 K for 6 h. The as-prepared Ni/MCM-41(TIE) catalyst precursor was collected by hot filtration, followed by thorough washing with ethanol to remove the unbound metal ions on the surface of MCM-41. The remaining organic template was expelled by calcination at 823 K for 2 h in Ar flow. The reduction procedure was carried out in a 25% H_2/Ar flow at 973 K for 2 h. The KOH-modified catalyst was prepared similarly to the metal/MCM-41(TIE) and is designated as K-Ni/MCM-41(TIE). Inductively coupled plasma–atomic emission spectrometry (ICP-AES) measurements showed that the actual loading of Ni was 7.2 wt%.

2.2. Catalytic testing

Catalytic testing was carried out in a continuous-flow quartz reactor (catalyst: 100 mg, 60–80 mesh) under pure NH_3 (flow rate: 50 ml/min; $GHSV_{NH_3}$: 30,000 ml/(h g_{cat})). Before the reaction, the catalyst was reduced in situ in a 25% H_2/Ar flow at 823 K for 2 h, then purged with a flow of pure Ar. The reaction temperature was in the range of 623–993 K. The acquisition of activity data at a particular temperature was conducted after the establishment of steady state. Product analysis was performed on an on-line gas chromatograph (Shimadzu) equipped with thermal detector and Poropak Q column, using Ar as a carrier gas. NH_3 conversion in a blank reactor was $<1.0\%$ at 823 K.

2.3. Characterization

Powder XRD experiments was conducted on a Rigaku Automatic diffractiometer (Rigaku D-MAX) with monochromatized Cu-K_α radiation ($\lambda = 0.15406$ nm) at a setting of 30 kV. A JEM-2010F TEM device was used (at 200 kV) to investigate the morphology and particle size of the catalysts. The amount of Ni loading in the Ni/MCM-41(TIE) catalyst was validated on an American JA-1100 type ICP-AES instrument. The BET surface areas and pore structures were measured with a NOVA-1200 Material Physical Structure Determinator. The samples were degassed at 573 K for 3 h, then N_2 adsorption was conducted at 77 K. H_2 TPR and TPD experiments were conducted as described previously [33], with sample sizes of 40 mg for TPR and 0.2 g for TPD.

3. Results

3.1. Physical properties

The mesostructure features of the three support materials were verified by small-angle XRD patterns and N_2 adsorption–desorption measurements. MCM-41 and SBA-15 showed typical mesoporous structures in accordance with those reported in the literature [38–40], whereas fumed SiO_2 is essentially nonporous.

Table 1 reports the physical characteristics of the support materials and the supported metal catalysts. It is apparent that the loading of active component has a notable impact on the surface area of mesoporous MCM-41 and SBA-15, but not as much on that of nonporous fumed SiO_2. The specific surface area and pore volume of MCM-41 dropped appreciably with metal loading and decreased further with KOH modification. The slight decrease in average pore size indicated that significant amount of active component had entered the pores. When SBA-15 was loaded with an active component, the specific surface area and pore volume decreased more notably than that of the MCM-41 case, and, interestingly, average pore size increased. Surely, the large pores of SBA-15 can provide more

Table 1
The physical properties of supports and supported metallic catalysts

Catalyst[a]	S_{BET} (m^2/g)	Pore volume (cm^3/g)	Pore diameter (Å)
MCM-41	991	0.92	37.0
SBA-15	762	0.96	50.4
Fumed SiO_2	260	–	–
Ru/MCM-41(IMP)	948	0.84	35.5
K-Ru/MCM-41(IMP)	816	0.69	34.0
Ru/SBA-15	616	0.78	50.3
K-Ru/SBA-15	415	0.59	56.9
Ru/fumed SiO_2	227	–	–
K-Ru/fumed SiO_2	203	–	–
Ni/MCM-41(IMP)	860	0.74	34.5
K-Ni/MCM-41(IMP)	742	0.60	32.3
Ni/MCM-41(TIE)	449	0.38	33.8
K-Ni/MCM-41(TIE)	297	0.25	33.5
Ni/SBA-15	389	0.58	59.8
K-Ni/SBA-15	334	0.52	63.4
Ni/fumed SiO_2	215	–	–
K-Ni/fumed SiO_2	189	–	–

[a] The metal catalysts not prepared by TIE method were all prepared by impregnation method.

space for access of more active components, producing a notable decrease in surface area and pore volume. Some existing micropores were preferably blocked by metal particles, and the apparent average pore size of SBA-15 increased appreciably with metal loading.

The surface area of the supported Ni catalyst is slightly lower than that of the corresponding supported Ru catalyst, signifying that the dispersions of the metal particles in the two cases are somewhat different. The surface area and pore volume of Ni/MCM-41(TIE) are only about half those of Ni/MCM-41(IMP), but there is little difference in pore size between the two. It is possible that the TIE method had a considerable effect on the structural character of the support.

3.2. Catalytic activity

Table 2 gives the NH_3 conversion and H_2 formation rates over supported Ru catalysts. One can see that the Ru catalysts prepared in this study are more active than the 10% Ru/SiO_2 of ordinary silica support reported previously [7]. Both catalysts were evaluated under identical conditions. The results clearly illustrate that the nature of support material plays an important role in determining the activity of metal catalysts. It was previously reported that alkali or alkaline earth metal ions are efficient promoters for supported Ru or Fe catalysts in NH_3 synthesis and decomposition; they are also effective adjuvants for preventing Ru or Fe from sintering [19,30]. As shown in Table 2, KOH modification leads to increased catalytic activity for all catalysts. The effect of KOH modification becomes most significant over Ru supported on MCM-41 at reaction temperatures above 450 °C. Over K-Ru/MCM-41, K-Ru/fumed SiO_2, and K-Ru/SBA-15, almost 100% ammonia conversion can be achieved above 550 °C. The corresponding H_2 formation rates achieved on these three catalysts at 500 °C were 29.41, 27.61, and 26.51 mmol/(min g_{cat}), respectively, much higher than that (20.0 mmol/(min g_{cat})) achieved over 10% Ru/SiO_2 at equal temperature [7].

Table 3 depicts the NH_3 conversion and H_2 formation rates over supported Ni catalysts of the current study. Similarly, NH_3 conversion was much higher than that achieved over 10% Ni/SiO_2 with ordinary silica as a support [7]. At 600 °C, NH_3 conversion achieved over Ni/MCM-41(IMP) was almost twice that achieved over 10% Ni/SiO_2 [7]. It is noteworthy that the nickel catalysts supported on the three siliceous ma-

Table 2
H_2 formation rate (mmol/(min g_{cat})) and NH_3 conversion (data in parentheses, %) over the supported Ru catalysts

Temperature (°C)	Ru/*support*			K-Ru (2:1)/*support*			10% Ru/SiO_2 Ref. [7]
	Fumed SiO_2	MCM-41	SBA-15	Fumed SiO_2	MCM-41	SBA-15	
400	7.6 (22.6)	6.9 (20.5)	9.2 (27.6)	11.0 (32.7)	11.3 (33.8)	11.8 (35.4)	4.5 (14.3)
450	16.7 (49.7)	14.2 (42.4)	16.4 (49.0)	19.0 (56.6)	20.4 (60.9)	19.4 (57.9)	11.4 (36.4)
470	20.3 (60.7)	18.4 (54.9)	19.8 (59.3)	22.6 (67.5)	26.4 (78.9)	22.4 (66.8)	–
500	26.2 (78.1)	23.9 (71.3)	24.6 (73.4)	27.6 (82.5)	29.4 (87.8)	26.5 (79.2)	20.0 (64.0)
520	29.2 (87.3)	27.5 (82.1)	27.7 (82.7)	29.9 (89.3)	31.6 (94.4)	29.3 (87.4)	–
550	32.3 (96.5)	31.7 (94.6)	31.2 (93.3)	32.7 (97.7)	33.5 (100.0)	32.0 (95.5)	–

Table 3
H_2 formation rate (mmol/(min g_{cat})) and NH_3 conversion (data in parentheses, %) over the supported Ni catalysts

Temperature (°C)	Ni/*support*				K-Ni (2:1)/*support*				10% Ni/SiO_2 Ref. [7]
	Fumed SiO_2	MCM-41 (IMP)	MCM-41 (TIE)	SBA-15	Fumed SiO_2	MCM-41 (IMP)	MCM-41 (TIE)	SBA-15	
400	1.5 (4.6)	2.7 (8.0)	2.1 (6.3)	2.8 (8.2)	2.28 (6.8)	2.9 (8.6)	3.2 (9.5)	3.2 (9.5)	0.44 (1.4)
450	3.5 (9.4)	4.7 (14.1)	4.0 (11.9)	4.0 (12.0)	4.52 (13.5)	4.9 (14.5)	5.7 (17.0)	4.4 (13.2)	1.3 (4.2)
500	6.5 (18.1)	9.0 (26.9)	8.9 (26.5)	7.3 (22.0)	8.37 (25.0)	8.9 (26.5)	10.7 (31.9)	7.7 (22.9)	3.3 (10.5)
550	11.6 (34.6)	14.9 (44.6)	15.9 (47.6)	12.7 (37.8)	14.28 (42.6)	15.0 (44.9)	17.3 (51.8)	12.9 (38.4)	6.8 (21.6)
600	18.0 (53.7)	21.5 (64.2)	24.0 (71.6)	19.2 (57.3)	20.77 (62.0)	21.8 (65.1)	24.5 (73.2)	19.3 (57.8)	11.4 (36.4)
650	25.1 (75.0)	27.9 (83.2)	30.6 (91.5)	25.6 (76.6)	27.28 (81.5)	28.2 (84.2)	31.1 (92.8)	26.4 (78.7)	21.1 (70)
670	27.7 (82.6)	29.8 (89.1)	32.1 (95.7)	28.2 (84.1)	29.78 (88.9)	30.3 (90.4)	32.5 (97.0)	28.8 (85.9)	–
700	31.3 (93.4)	32.0 (95.4)	33.1 (98.8)	31.3 (93.6)	32.06 (95.7)	32.8 (97.8)	33.5 (100)	31.8 (94.9)	–

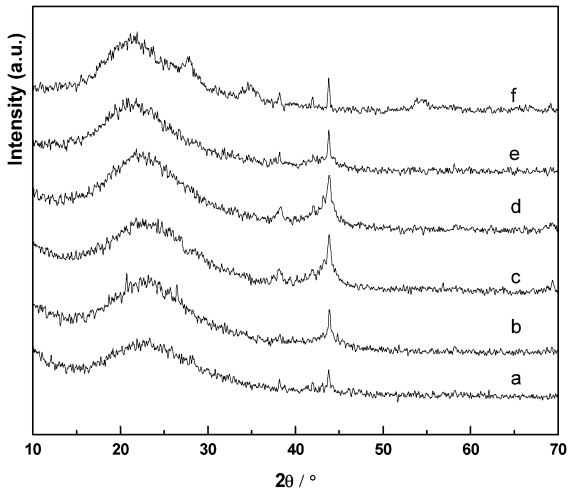

Fig. 1. XRD patterns of supported Ru catalysts: (a) Ru/MCM-41; (b) K-Ru/MCM-41; (c) Ru/SBA-15; (d) K-Ru/SBA-15; (e) Ru/fumed SiO_2; (f) K-Ru/fumed SiO_2.

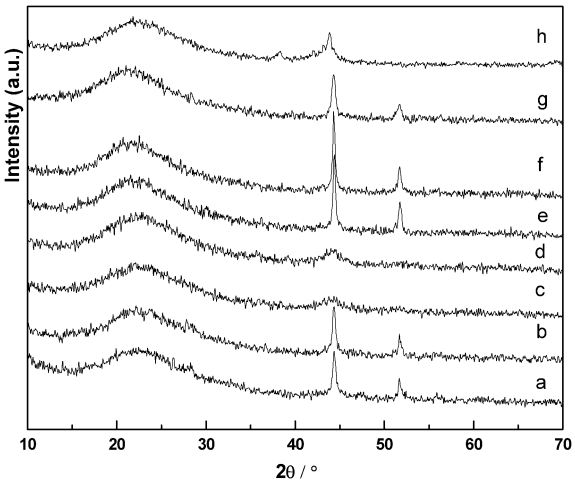

Fig. 2. XRD patterns of supported Ni catalysts: (a) Ni/MCM-41(IMP); (b) K-Ni/MCM-41(IMP); (c) Ni/MCM-41(TIE); (d) K-Ni/MCM-41(TIE); (e) Ni/SBA-15; (f) K-Ni/SBA-15; (g) Ni/fumed SiO_2; (h) K-Ni/fumed SiO_2.

terials were also more active than that supported on CNTs [30–34]. The H_2 formation rates at 500 °C for the Ni catalysts supported on MCM-41, SBA-15, and fumed SiO_2 were 9.00, 7.35, and 6.05 mmol/(min g_{cat}), respectively, compared with a value of 2.90 mmol/(min g_{cat}) for Ni/CNTs [31]. Furthermore, the Ni/MCM-41(TIE) catalyst was more active than Ni/MCM-41(IMP), probably owing to higher Ni dispersion (see Table 4 later). The effect of KOH modification on nickel catalysts was also investigated. The catalyst supported on fumed SiO_2 showed a certain improvement in activity, but only slight changes were observed over the catalysts supported on MCM-41 and SBA-15. Thus it follows that the effect of potassium modification varies depending on the active components and supports.

3.3. Metal dispersion

Fig. 1 shows the XRD patterns of reduced Ru catalysts. All samples exhibit broad diffraction peaks of siliceous materials. Compared with the SBA-15 sample, the MCM-41 and fumed SiO_2 samples demonstrate weaker diffraction lines attributable to crystalline Ru particles ($2\theta = 43.86°$), signifying relatively higher Ru dispersion. The larger pore size of SBA-15 means more space and better accommodation for active components, which may favor the formation of bulk-like species. There are no obvious changes in KOH modification. As suggested by Ying et al. [34], the potassium might still remain as KOH, because the corresponding oxide phase is unfavorable in the presence of water produced during the reduction process.

Fig. 2 reports the XRD patterns of the reduced Ni catalysts. Diffraction lines attributable to crystalline Ni particles ($2\theta = 44.25°, 51.8°$) are clearly visible for all samples prepared by the impregnation method. The Ni diffraction signal can hardly be identified for Ni/MCM-41(TIE). Considering the 7.2 wt% Ni loading of Ni/MCM-41(TIE) and 5.0 wt% Ni loading of Ni/MCM-41(IMP), the TIE method enables greater Ni dispersion. It follows that due to ion exchange between Ni and template ions, the supported Ni components were located

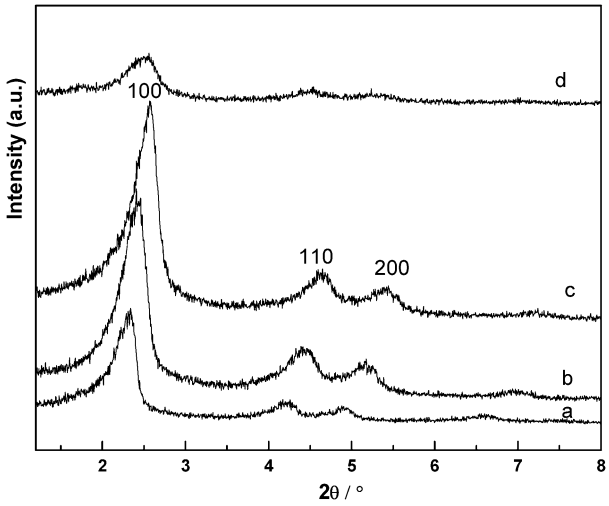

Fig. 3. Small angle XRD patterns of MCM-41 and supported Ni catalysts via different preparation methods: (a) MCM-41, as prepared; (b) MCM-41, after calcination; (c) Ni/MCM-41(IMP); (d) Ni/MCM-41(TIE).

mainly on the pore wall of MCM-41 and retained in much smaller sizes.

Fig. 3 shows the small-angle XRD patterns of the as-prepared MCM-41, calcined MCM-41, Ni/MCM-41(TIE), and Ni/MCM-41(IMP) samples. The XRD diffraction lines of the four samples can be indexed to hexagonal regularity of MCM-41 pore structure, that is, (100), (110), and (200) planes. The (100) peak of calcined MCM-41 and Ni/MCM-41(IMP) is more intense, because of removal of the template. The peak intensity of Ni/MCM-41(TIE) is much weaker than those of the other samples; we deduce that even though the mesoporous pore structure of MCM-41 was not largely destroyed in the TIE method, the long-range order of the hexagonally ordered porosity may be significantly lowered, which also accounts for a considerable decrease in the surface area of this sample (Table 1).

Figs. 4 and 5 depict the N_2 adsorption–desorption isotherms and pore size distributions of MCM-41, Ni/MCM-41(TIE), and

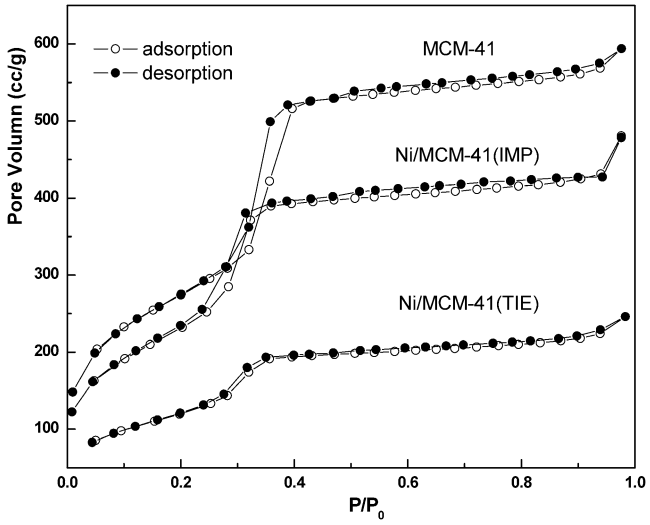

Fig. 4. Nitrogen adsorption and desorption isotherms of MCM-41, Ni/MCM-41(TIE) and Ni/MCM-41(IMP).

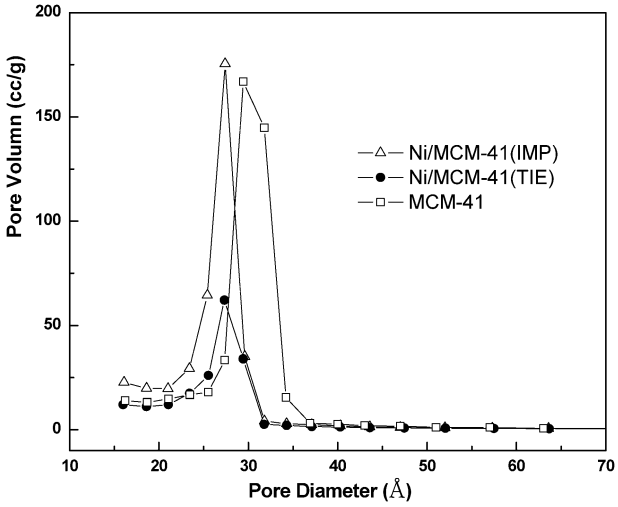

Fig. 5. Pore distribution of MCM-41, Ni/MCM-41(TIE) and Ni/MCM-41 (IMP).

Ni/MCM-41(IMP). The samples show type IV hysteresis loop isotherms with a sudden increase within the P/P_0 range of 0.3–0.4, signifying that the mesoporous pore structures would be largely maintained in both loading methods. However, the pore volume of MCM-41 was greatly reduced with Ni loading, especially in the Ni/MCM-41(TIE) case. The results of pore size distribution indicate uniform pore size and a ca. 4 Å decrease in average pore size of the sample with Ni loading.

3.4. Metal–support interaction

Fig. 6 reports the TPR profiles of Ru and Ni precursors supported on MCM-41. The metal oxides (NiO and RuO_2) could be completely reduced below 850 °C. It can be seen that the impregnated Ni precursor is the most difficult to reduce (Fig. 6, a). The temperature for Ni/MCM-41(TIE) reduction is notably lower than that for Ni/MCM-41(IMP) reduction. This

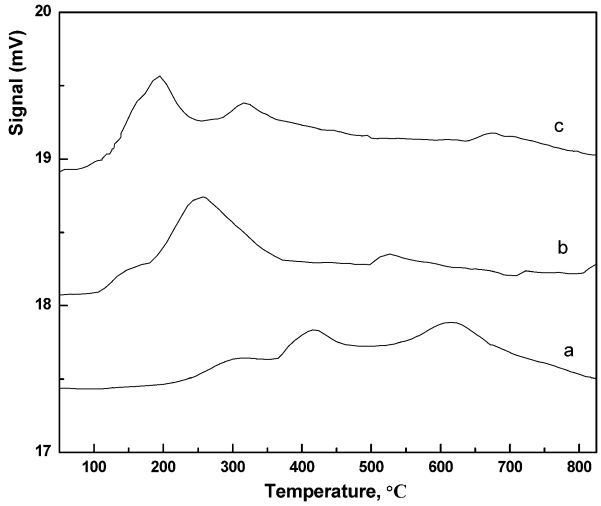

Fig. 6. H_2-TPR profiles of precursors: (a) Ni/MCM-41(IMP); (b) Ni/MCM-41(TIE); (c) Ru/MCM-41(IMP).

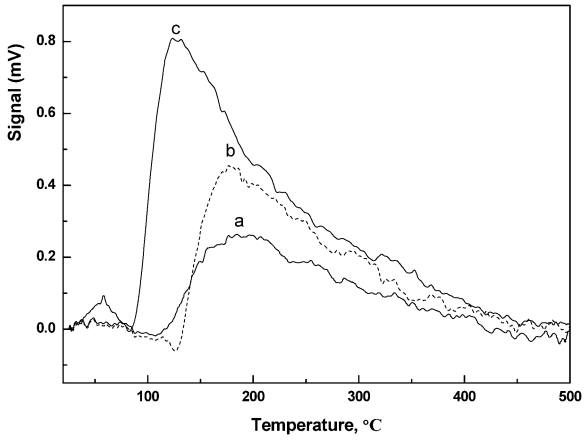

Fig. 7. H_2-TPD profiles of MCM-41 supported Ni and Ru catalysts: (a) K-Ru/MCM-41(IMP); (b) K-Ni/MCM-41(IMP); (c) K-Ni/MCM-41(TIE).

can be ascribed to weaker interaction of Ni component with support and/or to smaller size of the metal particles.

Fig. 7 illustrates the H_2 desorption behaviors of the K-Ni/MCM-41(IMP), K-Ni/MCM-41(TIE), and K-Ru/MCM-41 (IMP) catalysts. (H_2 adsorption on pure MCM-41 is insignificant.) The H_2-desorption profiles of K-Ru/MCM-41(IMP) and K-Ni/MCM-41(IMP) are quite similar, the desorption temperatures are ca. 70 K lower than that of the K-Ru/CNTs—a catalyst reported by Yin et al. [33]. However, Ni loading with the TIE method resulted in a notable decrease in both onset temperature and peak temperature (ca. 50 K shift to the lower-temperature end). The amount of H_2 desorption over K-Ni/MCM-41(TIE) was almost twice as that over K-Ni/MCM-41(IMP), indicated that the former has more exposed surface Ni atoms.

Based on the peak area of the H_2-TPD profiles and assuming an adsorption of one H atom per metal atom [7], the H_2 chemisorption uptakes can be estimated accordingly as calibrated by a standard procedure of CuO reduction. As shown in Table 4, H_2 chemisorption uptake over K-Ni/MCM-41(IMP) is roughly 42.5 μmol/g_{cat}, slightly higher than that over K-Ru/MCM-41(IMP) (34.1 μmol/g_{cat}), but lower than that

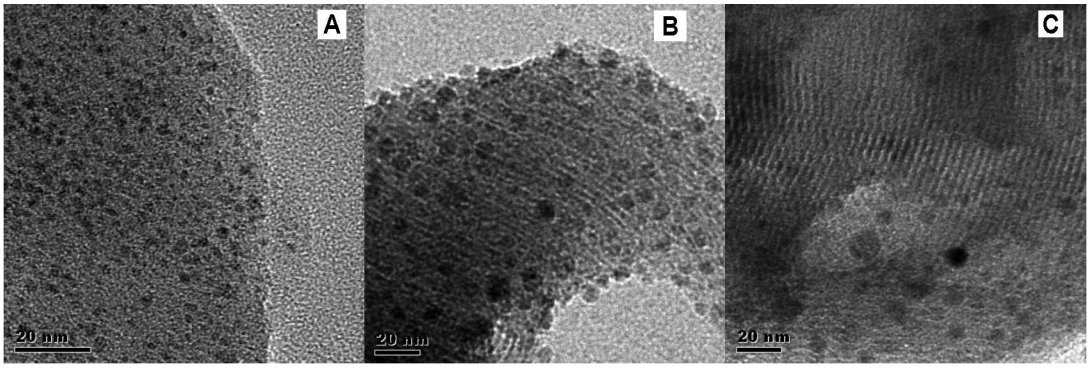

Fig. 8. TEM images of catalysts: (A) Ru/MCM-41(IMP); (B) Ni/MCM-41(IMP); (C) Ni/MCM-41(TIE).

over K-Ru/CNTs (51.4 μmol/g_{cat}) [33]. The H_2 chemisorption uptake of K-Ni/MCM-41(TIE) (89.2 μmol/g_{cat}) was twice that of K-Ni/MCM-41(IMP). The dispersions of metal components were 14.4% for K-Ni/MCM-41(TIE), 9.9% for K-Ni/MCM-41(IMP), and 13.8% for K-Ru/MCM-41(IMP), much higher than the values of 0.9% for 10% Ni/SiO_2 and 1.2% for 10% Ru/SiO_2 reported by Choudhary et al. [7].

3.5. Particle size of metal components

We used the TEM technique to investigate the effects of support and loading method on the particle size and morphology of catalysts. As shown in Fig. 8A, the Ru particles are spherical and evenly dispersed on MCM-41. The mean particle size was estimated by averaging the diameter of 100 randomly distributed particles; it was approximately 5 nm for Ru metal particles. TEM image of Fig. 8B clearly shows that the dispersion level of Ni particles on MCM-41 is indeed lower than that of Ru. This observation is consistent with the results of XRD and H_2 chemisorption measurements. It is obvious that Ni aggregation to larger particles (ca. 8 nm) occurred. Besides the difference in intrinsic chemical nature between Ni and Ru, the relatively lower dispersion may also account for the lower activity of Ni in ammonia decomposition. Comparing with the TEM image of Ni/MCM-41(IMP), that of Ni/MCM-41(TIE) (Fig. 8C) shows fewer Ni particles were on the outer surface of MCM-41, implying that a larger amount of Ni was located inside the pores of the support.

4. Discussion

4.1. Turnover frequency and structure sensitivity

The turnover frequency (TOF) of the reaction over different catalysts was calculated by normalizing the observed reaction rate (mol H_2/(s g_{cat})) to the number of exposed Ru or Ni surface atoms per gram of catalyst. The TOF value derived on the K-Ru catalyst was much higher than that derived on the Ni-based catalysts (Fig. 9). For the Ni-based catalysts, the TOF value of K-Ni/MCM-41(TIE) was lower than that of K-Ni/MCM-41(IMP), despite the fact that the former is actually more active on the basis of per unit mass of catalyst. The difference in TOF values between the Ru and Ni catalysts can

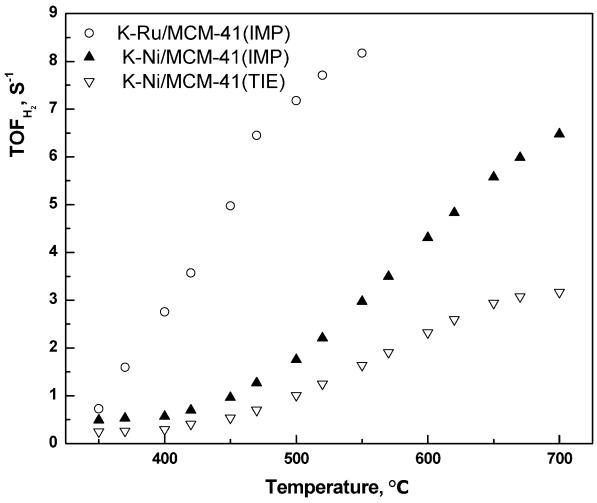

Fig. 9. Comparison of TOFs of H_2 formation over MCM-41 supported K-Ni and K-Ru catalysts.

be attributed mainly to their intrinsic chemical natures; whereas the difference in TOF values between the Ni catalysts prepared by different methods should be ascribed to the changes in Ni dispersion and, consequently, to the changes in morphology and structure of Ni particles.

It is generally accepted that at metal surfaces, the "active sites" with low-coordination atoms are more reactive [41]. The current studies on ammonia synthesis/decomposition were focused mainly on Fe and Ru systems [42–44] and less on Ni-based catalysts. For the Fe catalysts, the active sites associated with N_2 dissociation in ammonia synthesis were thought to be the oligo-atomic metal clusters, that is, the C-7 sites (with seven nearest neighbors) [42]; for the Ru catalysts, the B5 sites (with five nearest neighbors) were proposed [43,44]. The results of DFT calculations suggested that B5 sites can be the five-member sites on the steps of the Ru(0001) plane [43]. Because of their unique geometry configuration and electronic properties, the B5 sites can favor both dissociation and desorption of N_2 at the steps of the Ru(0001) face rather than at the terraces [44].

The constitution of such active sites is very structure-sensitive; in other words, the concentration of these unique sites is strongly dependent on metal dispersion or particle size. Recent work on a series of Ru/C catalysts with different Ru

Table 4
H_2-TPD results of MCM-41 supported K-Ni and K-Ru catalysts for ammonia decomposition

Sample	H_2-TPD				E_a[b] (kJ/mol)
	Onset desorption temperature (°C)	H_2 uptake (μmol/g_{cat})	Peak temperature (°C)	Dispersion[a] (%)	
K-Ni/MCM-41(TIE)	84	89.2	126	14.4	49.3
K-Ni/MCM-41(IMP)	125	42.5	176	9.9	53.5
K-Ru/MCM-41(IMP)	107	34.1	178	13.8	49.7

[a] Dispersion was estimated according to H_2 uptake, assuming molar ratio of Ru:H = 1:1.
[b] Apparent activation energy was obtained from the corresponding Arrhenius plots in Fig. 10.

loadings revealed that Ru particle size increased monotonously with increasing Ru content [45]. At Ru loading <3 wt%, the Ru particles were smaller than 0.7–0.8 nm and catalytically inactive for ammonia synthesis. This is because less B5 active sites were present on these extremely fine Ru particles. The maximum concentration of B5 sites was observed over the Ru crystallites of ∼2 nm size. Another study of ammonia synthesis on Ru/C catalysts [46] showed that the optimal Ru loading was ca. 3.5 wt%, with Ru dispersion of 10–15% very close to the values of Ni dispersion (9.9–14.4%) reported in the present study. Too high a dispersion (>15%) would result in a reduction of B5 sites and consequently lower catalytic activity. But Ru loading beyond a certain amount also was not helpful, because heavy Ru loading simply increased the particle size but did not effectively increase the number of B5 sites. Jacobsen et al. [47] found significantly increased activity over Ru catalysts supported on magnesium aluminium spinel during the initial period of ammonia synthesis. This activity increase was ascribed to sintering of very small Ru particles (<1 nm) to medium Ru crystals. All of these observations strongly suggest that the concentration of B5 sites is closely related to the metal particle size. One should bear in mind that in these studies, the adopted supports are different, and the procedures for catalyst characterization and evaluation are not identical; thus the optimal dispersion can vary somewhat even for the same supported metal component.

In the present study, the TOF values derived on the Ni-based catalysts for ammonia decomposition changed significantly with varying levels of Ni dispersion. It follows that ammonia decomposition over Ni catalysts is also very structure-sensitive, and that a relationship between the number of active sites and the Ni dispersion (particle size) can also be established. The B5-like sites are proposed to be active for ammonia decomposition on the surfaces of Ni particles. For the K-Ni/MCM-41(TIE) catalyst, the Ni component is located mainly on the internal wall of MCM-41 and has an extremely fine particle size. Although the metal dispersion is higher, less active sites are present on these very fine Ni particles, leading to a considerable decrease in TOF values. It should be mentioned that the morphology of metal crystallites changes simultaneously with metal dispersion (particle size), which in turn influences the constitution of unique active sites. A previous study on Ru catalysts [48] revealed that at low Ru loading, the small Ru particles (∼2 nm) are spherical, whereas at higher loadings, the exposed faces of larger Ru crystallites are essentially flat. There were more B5 sites present on the latter planes, beneficial for the reaction. Because

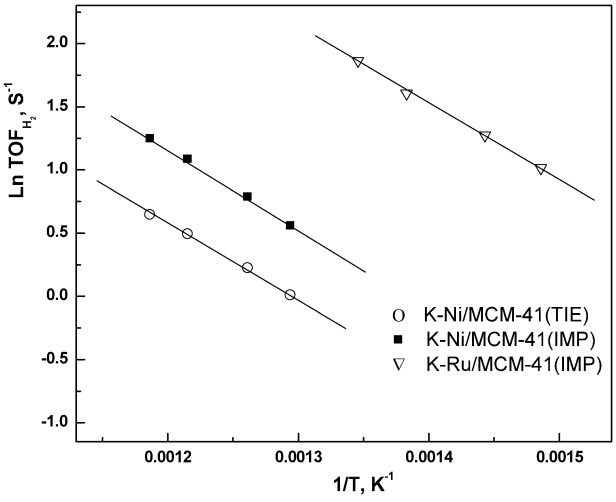

Fig. 10. The Arrhenius plots over MCM-41 supported K-Ni and K-Ru catalysts. The temperature range adopted for K-Ni/MCM-41(TIE) and K-Ni/MCM-41(IMP) was 808 ± 35 K, at NH_3 conversions of 45 ± 15% and 40 ± 15%, respectively. The temperature range adopted for K-Ru/MCM-41 (IMP) was 708 ± 35 K, at NH_3 conversions of 50 ± 17%.

of the difference in Ni dispersion between K-Ni/MCM-41(TIE) and K-Ni/MCM-41(IMP), the morphology of Ni particles can also be envisaged to change. In K-Ni/MCM-41(IMP), there are larger Ni crystallites and hence flatter faces, on which more B5-like sites are probably present, resulting in a higher TOF in NH_3 decomposition. A correlation between metal dispersion (particle size) and TOF for NH_3 decomposition has been observed by other investigators. For instance, Choudhary et al. [7] investigated ammonia decomposition over Ni, Ir, and Ru catalysts supported on different materials. A common observation was that for a certain metal component, TOF decreased with increasing metal dispersion. Liang et al. [49] observed that the TOF value over a Ru catalyst supported on activated carbon increased by a factor of 9 when the size of Ru particles increased from 1.7 to 10.3 nm. Yin et al. [33] also observed similar phenomenon on the Ru catalysts supported on CNTs.

4.2. Activation energy

From the Arrhenius plots in Fig. 10 based on the H_2 formation data far away from the equilibrium value, we obtained the related apparent activation energies (E_a); the results are listed in Table 4. The E_a values are estimated from the integral reaction rates obtained at SV = constant and at typical NH_3 conversions, for example, at 45 ± 15% and 40 ± 15% NH_3 con-

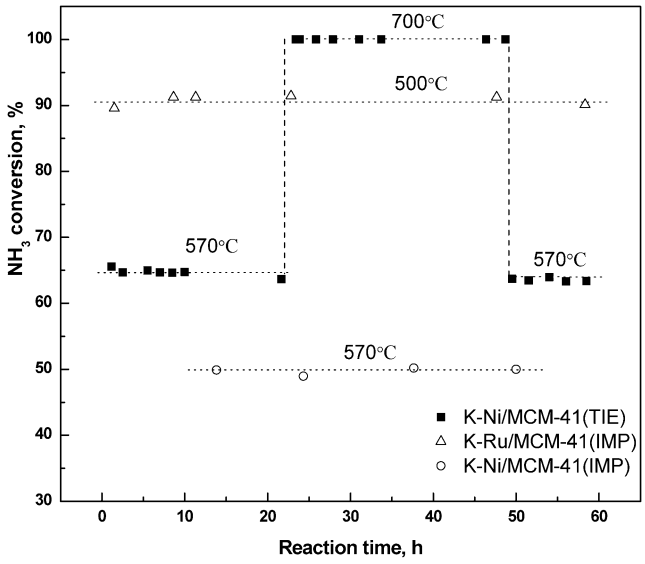

Fig. 11. stability study of K-Ni/MCM-41(TIE), K-Ni/MCM-41(IMP), and K-Ru/MCM-41(IMP).

versions for K-Ni/MCM-41(TIE) and K-Ni/MCM-41(IMP), respectively. The E_a value for K-Ru/MCM-41(IMP) was also estimated similarly. It is believed that the E_a values obtained in such a way are still meaningful and are not influenced significantly by mass transfer limitations. If one compared the E_a value of K-Ni/MCM-41(IMP) (53.5 kJ/mol, see Table 4) with that of Ni/CNTs (90.3 kJ/mol) [31], one can conclude that the E_a value derived in the present study is reasonable because the former catalyst is indeed more active than the latter. It is also evident that loading method of Ni has a great influence on the activation energy of the supported Ni catalysts; the E_a value of K-Ni/MCM-41(IMP) was 53.5 kJ/mol, whereas that of K-Ni/MCM-41(TIE) was 49.3 kJ/mol. Both values are lower than that (varied from 20 to 22 kcal/mol) reported for 10% Ni/SiO_2, 10% Ni/HY, 10% Ni/HZSM-5, and 65% Ni/SiO_2/Al_2O_3 [7], and also much lower than the values (43 kcal/mol) reported for Ni films [50] and Ni wires (50 kcal/mol) [51].

4.3. Catalyst stability

Fig. 11 clearly shows that the catalysts of K-Ni/MCM-41 (TIE), K-Ni/MCM-41(IMP), and K-Ru/MCM-41(IMP) showed excellent stability under applied reaction conditions. The K-Ni/MCM-41(TIE) catalyst did not show any loss in NH_3 conversion even after a reaction period of >20 h at 700 °C. In contrast, the carbon-supported catalysts are unstable (due to methanation) in the presence of H_2 in both NH_3 synthesis and decomposition [34,46,52]. It was reported that the rate of CNT methanation was rather notable (1.3×10^2 unit/K) at 427 °C, a common temperature applied for NH_3 decomposition [34]. Although the resistance to carbon methanation can be enhanced with the pretreatment of carbon or the modification of alkali or alkaline earth metal salts, degradation of carbon-supported catalysts is usually inevitable. Therefore, the present Ru and Ni catalysts supported on MCM-41 are thermally more stable and have better prospects for practical applications.

5. Conclusion

Adopting fumed SiO_2, MCM-41, and SBA-15 as catalyst supports, highly active Ru and Ni catalysts have been fabricated for the generation of CO_x-free H_2 from ammonia. The Ru catalysts were more active than the corresponding Ni catalysts. Modification of Ru catalysts with KOH led to significant activity enhancement; however, KOH modification of Ni catalysts did not result in any significant change in catalytic activity. Among the Ru and Ni catalysts, the KOH-modified Ru/MCM-41 and Ni/MCM-41 are the most active. Thus, of the three siliceous materials, MCM-41 is the most suitable for supporting Ru and Ni for ammonia decomposition.

The Ni component loaded on MCM-41 by the TIE method is located largely inside the pores of support and exhibited appropriate dispersion and higher catalytic activity than that loaded by conventional impregnation method. According to the deviations in metal dispersion and TOF between K-Ni/MCM-41(TIE) and K-Ni/MCM-41(IMP), it was demonstrated that NH_3 decomposition over the supported Ni catalysts is also significantly structure-sensitive. Preparation methodology can have a considerable effect on metal dispersion and thus change the catalytic performance of a catalyst. In view of the superior catalytic activity and high thermal stability, the MCM-41-supported Ru and Ni catalysts are promising candidates for practical applications.

References

[1] A.S. Chellappa, C.M. Fischer, W.J. Thomson, Appl. Catal. A 227 (2002) 231.
[2] R.O. Idem, N.N. Bakhshi, Ind. Eng. Chem. Res. 33 (1994) 2047.
[3] T.V. Choudhary, D.W. Goodman, Catal. Lett. 59 (1999) 93.
[4] T.V. Choudhary, D.W. Goodman, J. Catal. 192 (2002) 316.
[5] V.R. Choudhary, B.S. Uphade, A.S. Mamman, J. Catal. 172 (1997) 281.
[6] J.N. Armor, Appl. Catal. A 176 (1999) 159.
[7] T.V. Choudhary, C. Svadinaragana, D.W. Goodman, Catal. Lett. 72 (2001) 197.
[8] W. Rarog, Z. Kowalczyk, J. Sentek, D. Skladanowski, D. Szmigiel, J. Zielinski, Appl. Catal. A 208 (2001) 213.
[9] W. Raróg, D. Szmigiel, Z. Kowalczyk, S. Jodzis, J. Zielinski, J. Catal. 218 (2003) 465.
[10] A. Jedynak, Z. Kowalczyk, D. Szmigiel, W. Raróg, J. Zielinski, Appl. Catal. A 237 (2002) 223.
[11] D.A. Goetsch, S.J. Schmit, WO Patent 0 187 770 (2001).
[12] K. Kordesch, V. Hacker, R. Fankhauset, G. Faleschini, WO Patent 0 208 117 (2002).
[13] M.E.E. Abashar, Y.S. Al-Sughair, I.S. Al-Mutaz, Appl. Catal. A 236 (2002) 35.
[14] R.Z. Sorensen, L.J.E. Nielsen, S. Jensen, O. Hansen, T. Johannessen, U. Quaade, C.H. Christensen, Catal. Commun. 6 (2005) 229.
[15] S.F. Yin, B.Q. Xu, X.P. Zhou, C.T. Au, Appl. Catal. A 277 (2004) 1.
[16] R. Metkemeijer, P. Achard, Int. J. Hydrogen Energy 19 (1994) 535.
[17] R. Metkemeijer, P. Achard, J. Power Sources 49 (1994) 271.
[18] W. Arabczyk, J. Zamlynny, Catal. Lett. 60 (1999) 167.
[19] W. Arabczyk, U. Narkiewicz, Appl. Surf. Sci. 196 (2002) 423.
[20] J. Hepola, P. Simell, Appl. Catal. B 14 (1997) 287.
[21] P.A. Simell, J.O. Hepola, A.O. Krause, Fuel 76 (1997) 1117.

[22] G. Papapolymerou, V. Bontozoglou, J. Mol. Catal. A: Chem. 120 (1997) 165.
[23] J.G. Choi, J. Catal. 182 (1999) 104.
[24] K. Hashimoto, N. Toukai, J. Mol. Catal. A: Chem. 161 (2000) 171.
[25] M.C.J. Bradford, P.E. Fanning, M.A. Vannice, J. Catal. 172 (1997) 479.
[26] H. Dietrich, K. Jacobi, G. Ert, Surf. Sci. 352 (1996) 138.
[27] W. Arabczyk, J. Zamlynny, Catal. Lett. 60 (1999) 167.
[28] K. Kordesch, V. Hacker, R. Fankhauset, G. Faleschini, WO Patent 0 208 117 (2002).
[29] C. Boffito, J.D. Baker, WO Patent 9 840 311 (2002).
[30] S.F. Yin, B.Q. Xu, C.F. Ng, C.T. Au, Appl. Catal. B: Environ. 48 (2004) 237.
[31] S.F. Yin, Q.H. Zhang, B.Q. Xu, W.X. Zhu, C.F. Ng, C.T. Au, J. Catal. 224 (2004) 384.
[32] S.F. Yin, B.Q. Xu, S.J. Wang, C.F. Ng, C.T. Au, Catal. Lett. 96 (2004) 113.
[33] S.F. Yin, B.Q. Xu, W.X. Zhu, C.F. Ng, X.P. Zhou, C.T. Au, Catal. Today 93 (2004) 27.
[34] S.J. Wang, S.F. Yin, L. Li, B.Q. Xu, C.F. Ng, C.T. Au, Appl. Catal. B: Environ. 52 (2004) 287.
[35] G. Papapolymerou, V. Bontozoglou, J. Mol. Catal. A: Chem. 120 (1997) 165.
[36] M.C.J. Bradford, P.E. Fanning, M.A. Vannice, J. Catal. 172 (1997) 479.
[37] C.Y. Xiao, X. Chen, Z.Y. Wang, W.J. Ji, Y. Chen, C.T. Au, Catal. Today 93 (2004) 223.
[38] C.T. Kresge, M.E. Leonowicz, W.J. Roth, J.C. Vartuli, J.S. Beck, Nature 359 (1992) 710.
[39] J.S. Beck, L.C. Vartuli, W.J. Roth, M.E. Leonowicz, C.T. Kresge, K.D. Schmitt, C.T.W. Chu, D.H. Olson, E.W. Sheppard, S.B. McMullen, J.B. Higgings, J.C. Schlenker, J. Am. Chem. Soc. 114 (1992) 10834.
[40] D. Zhao, J. Feng, Q. Huo, N. Melosh, G.H. Fredrickson, B.F. Chmelka, G.D. Stucky, Science 279 (1998) 548.
[41] H.S. Taylor, Proc. R. Soc. London Ser. A 108 (1925) 105.
[42] J.A. Dumesic, H. Topsoe, M. Boudart, J. Catal. 37 (1975) 513.
[43] S. Dahl, A. Logadottir, R.C. Egeberg, J.H. Larsen, I. Chorkendorff, E. Tornqvist, J.K. Norskov, Phys. Rev. Lett. 83 (1999) 1814.
[44] S. Dahl, E. Tornqvist, I. Chorkendorff, J. Catal. 192 (2000) 381.
[45] W. Raróg-Pilecka, E. Miskiewicz, D. Szmigiel, Z. Kowalczyk, J. Catal. 231 (2005) 11.
[46] I. Rossetti, L. Forni, Appl. Catal. A 282 (2005) 315.
[47] C.J.H. Jacobsen, S. Dahl, P.L. Hansen, E. Tornqvist, L. Jensen, H. Topsoe, D.V. Prip, P.B. Moenshaug, I. Chorkendorff, J. Mol. Catal. A 163 (2000) 19.
[48] Z. Song, T.H. Cai, J.C. Hanson, J.A. Rodriguez, J. Hrbek, J. Am. Chem. Soc. 126 (2004) 8576.
[49] C.H. Liang, Z.B. Wei, Q. Xin, C. Li, Appl. Catal. A 208 (2001) 193.
[50] S.R. Logan, C. Kemball, Trans. Faraday Soc. 56 (1960) 144.
[51] R.W. McCabe, J. Catal. 79 (1983) 445.
[52] I. Rossetti, N. Pernicone, L. Forni, Catal. Today 102–103 (2005) 219.